

M. Orhan
N. S. Işık
T. Topal
M. Özer

Effect of weathering on the geomechanical properties of andesite, Ankara – Turkey

Received: 30 October 2005
Accepted: 6 January 2006
Published online: 14 February 2006
© Springer-Verlag 2006

M. Orhan · N. S. Işık (✉) · M. Özer
Department of Construction,
Geotechnical Division,
Gazi University, Besevler, 06500 Ankara,
Turkey
E-mail: nihatsinan@gazi.edu.tr

T. Topal
Department of Geological Engineering,
Middle East Technical University,
06531 Ankara, Turkey

Abstract Andesite exposed in different parts of Ankara has different weathering categories varying from fresh to residual soil. The geomechanical properties of the andesite are significantly affected by weathering. Buildings constructed especially in completely weathered and residual soil levels of the andesite have some geotechnical problems. In this study, the variation of the geomechanical properties of the andesite due to weathering is investigated in three selected sites of Ankara, through optical microscope, X-ray diffraction analyses, major element analyses, pressuremeter tests, physico-mechanical tests, and seismic refraction method. The data gathered from the field and laboratory studies were used to assess the characteristics of the weathering zones. Based on the data obtained from this study, an idealized weathering profile is assessed. No bearing capacity and consolidation settlement problems exist in the area. However, care should be taken for immediate settlement of the buildings. Slopes with heights less than 8 m are not expected to cause any significant problems for buildings. There exists a ground amplification problem in the study area. The natural period of the building should not match that of the weathered rock. The ground response analyses reveal that the buildings with four to seven stories may be adversely affected from earthquakes due to resonance phenomenon. Therefore, this has to be taken into account when designing new buildings.

Keywords Andesite · Ankara · Geomechanical properties · Weathering

Introduction

In the city of Ankara, various volcanic rocks of Miocene age such as andesite, tuff, and agglomerate are exposed. Among the volcanic rocks, the andesite covers a large area where rapid population growth is observed. However, different weathering categories ranging from fresh to residual soil can be observed within the andesite. The weathering adversely affects the geomechanical properties of the andesite giving rise to some geotechnical problems for buildings like shallow slope instability, ground amplification due to seismicity, bearing capacity,

and settlement. In order to overcome these problems, data on the variation of the geomechanical properties of the andesite due to weathering with depth are required.

The purpose of this study is to investigate the geomechanical properties of the weathered andesite. In order to accomplish these tasks, nine boreholes down to 20–25 m with a total length of 200 m were drilled at three different locations, namely Solfasol, Pursaklar, and Kecioren (Ovacık) districts of Ankara (Fig. 1). The samples taken from the boreholes were used to determine the depth of the weathering through major element analysis, X-ray diffraction analysis (XRD), standard

Geology

The capital of Turkey, Ankara is located in a basin trending ENE–WSW. The selected study sites are located within the metropolitan area. Andesite, agglomerate, and tuff exposed around the Ankara metropolitan area are of Miocene age. The distribution of the volcanic rocks in Ankara is shown in Fig. 2. The color of the andesite changes at different locations. According to Kasapoglu (1980), they are bluish gray, pink, and blackish violet. The andesite has a porphyritic texture with plagioclase and quartz phenocrysts embedded within a microlite matrix. The size of the phenocrysts ranges from 1 to 5 mm. Locally, yellowish beige dacite can be observed within the andesite. Although some researchers (Suludere 1976; Buyukonal 1971) indicated that hydrothermal alteration exists within the andesite, the weathering due to atmospheric effects is also dominant in the area (F. Arıkan,

Unpublished data). This study includes the effects of the weathering on andesite only, excluding the hydrothermal alteration.

The seismicity of Ankara and its vicinity is mainly controlled by the North Anatolian Fault Zone, which is a major right-lateral strike-slip fault that extends all the way from the North Aegean Sea toward East Anatolia over a distance of approximately 1,200 km with well-developed surface expression (Erdik et al. 1985). Ankara is approximately 100 km away from the fault zone. The distribution of epicenters for major earthquakes that occurred in the last 100 years with magnitudes greater than 4.0 is shown in Fig. 3 (USGS 2005). It indicates that the main source of earthquakes for the study area is the North Anatolian Fault Zone, although the faults at the southeast of Kırıkkale and southeast of Gölbaşı also form potential sources for earthquakes. Peak horizontal ground accelerations for the study area were calculated by various attenuation relationships using strike-slip fault mechanism and rock site conditions. The ground accelerations were calculated deterministically by adding one standard deviation to the results (Table 1). A value of 0.10 g for an area in Ankara was used by Teoman et al. (2004). Considering these acceleration values, 0.10 g which roughly corresponds to the upper bound of the calculated accelerations can be accepted as peak horizontal ground acceleration for the study area.

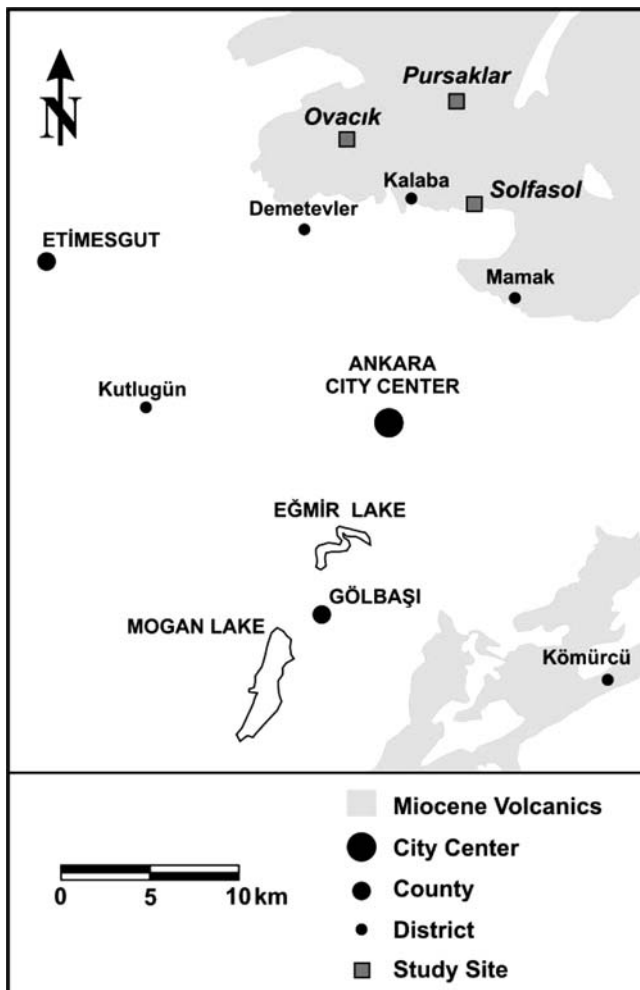


Fig. 2 Aerial distribution of the Miocene volcanics in Ankara

Depth and properties of the weathered andesite

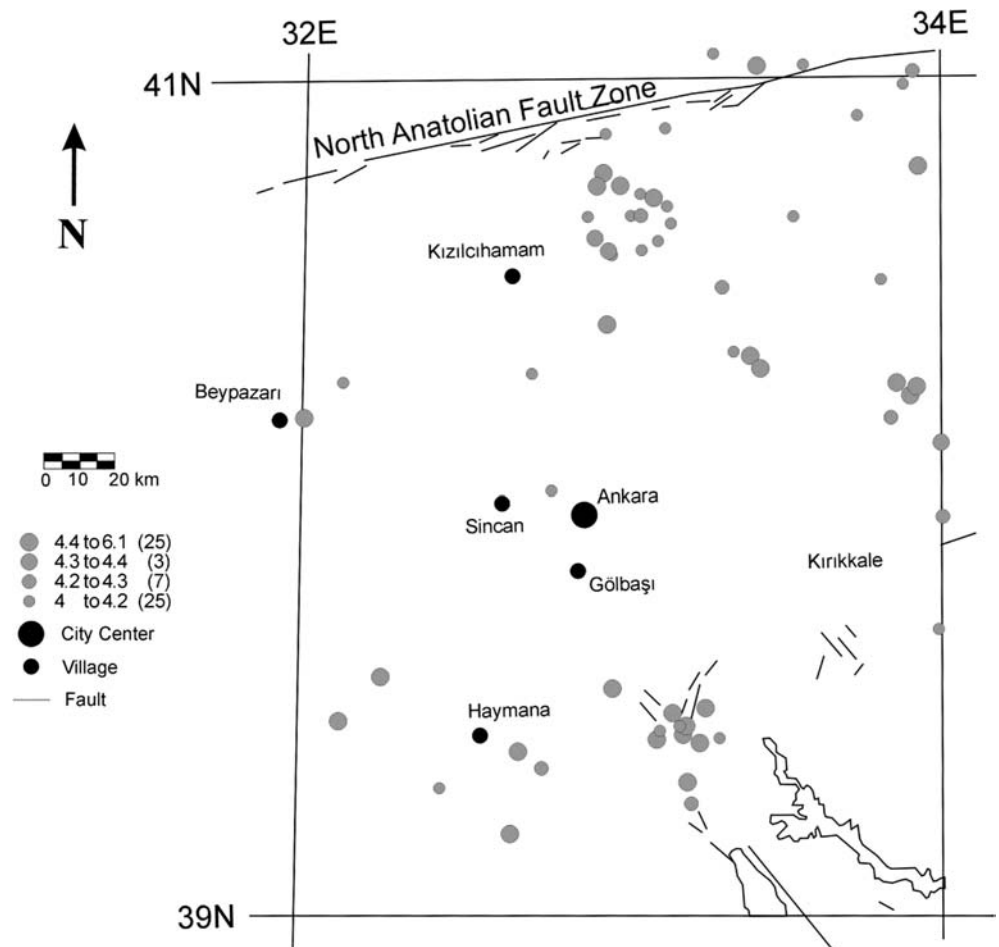
Physical and chemical weathering processes operating on the intact rock cause rocks to disintegrate physically and decompose chemically, forming new minerals. The processes also weaken the rocks. Therefore, optical microscopy, XRD technique, and chemical tests were used for the determination of the depth of the weathering. Additionally, the variation of the geomechanical properties of the rock was also investigated through pressuremeter tests, physicomchanical tests, and geophysical survey with seismic refraction method.

The complete weathering profile of the andesite is more clearly observed in the Pursaklar region. Approximately 0.5 m thick residual soil overlies the highly to completely weathered andesite (Fig. 4). Therefore, the andesite samples obtained only from this site were used for optical microscopy, XRD, and chemical tests with major element analysis. However, the geomechanical properties of the andesite were determined separately for each site.

Optical microscopy and XRD analyses

For the optical microscopy studies, a polarizing microscope was used. The andesite samples corresponding to

Fig. 3 The distribution of epicenters for major earthquakes that occurred in the last 100 years with magnitudes greater than 4.0 (USGS 2005)



2–3, 3–4, and 6–8 m depths were obtained for the thin sections. Based on the studies, the andesite from 2 to 3 m depth includes microlite matrix and phenocrysts of plagioclase and biotite with a small amount (< 5%) of quartz, opaque and calcite minerals. The microlite ma-

trix is almost sericitized and contains clay due to the weathering. Iron oxidation is also observed around the phenocrysts and along the cleavages of the minerals (Fig. 5). The samples taken from the deeper parts of the study area have similar mineralogy, but without iron oxidation. This indicates that the weathering is more effective down to 2–3 m depth.

X-ray diffraction analyses performed on the same samples reveal that smectite as an alteration product, feldspar, mica, quartz, hematite, and amorphous silica exist within the samples. The smectite content decreases with depth. XRD results are in good agreement with the optical microscopy findings.

Major element analyses

Chemical weathering of rocks may result in changes in initial elemental concentrations by leaching and enrichment (Borchardt et al. 1971; Borchardt and Harward 1971). A number of methods have been used to quantify the depths and degree of the chemical weathering of

Table 1 Peak horizontal ground acceleration values of the study area based on various attenuation relationships

Attenuation relationship by	Peak horizontal ground acceleration (g)
Sabetta and Pugliese (1987)	0.050
Campbell (1988)	0.100
Joyner and Boore (1988)	0.030
Fukushima and Tanaka (1990)	0.079
Abrahamson and Silva (1997)	0.076
Boore et al. (1997)	0.107
Sadigh et al. (1997)	0.060
Ulusay et al. (2004)	0.057



Fig. 4 Photograph of the weathering profile in the andesite of the Pursaklar region

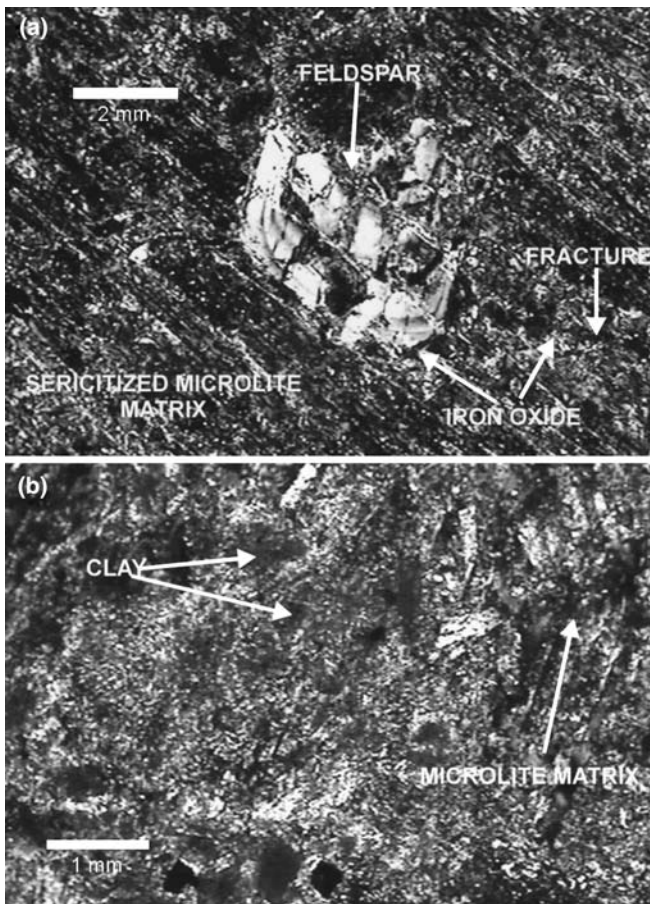


Fig. 5 Photomicrographs of the andesite, at 2–3 m depth, showing (a) sericitized microlite matrix, iron oxide, and altered feldspar, (b) clay within the microlite matrix

rocks (Martin 1986; Irfan 1999; Ng et al. 2001). However, chemical weathering may be quantified by using some chemical indices (Topal 2002). The indices mainly require major element analyses of weathered rocks. In order to determine the depth of chemical weathering, major element concentrations of the andesite were determined by means of the atomic absorption (Table 2). The depths of samples from the surface downwards were 0–1, 2–3, 3–4, and 6–8 m.

In this study, weathering potential index (WPI), product index (PI), Ruxton's ratio (R), Parker index (P), Vogt ratio (V), modified weathering potential index (MWPI), chemical index of alteration (CIA), lixiviation index (β), alumina to calcium–sodium oxide ratio (ACN), alumina to potassium–sodium oxide ratio (ALK), loss on ignition (LoI), mobiles index (I_{mob}), and mobility index (MI) are selected as chemical weathering indices. Additionally, cation exchange capacity (CEC) using methylene blue adsorption test (MBA) was also included for the quantification of the weathering depth because the chemical weathering of the andesite gives rise to the formation of clay minerals. For the MI calculations, Al_2O_3 is considered to be the stable constituent. A summary of the chemical weathering indices used in this study is given in Table 3. For ease of comparison among different chemical weathering indices, the analytical data are normalized so that all the indices have a value of 1 for the fresh andesite samples corresponding to a depth of 6–8 m. The relative contents (normalized values) of the chemical weathering indices of the andesite were plotted against depth in Fig. 6. Since the sampling points correspond to a range of depths (e.g., 6–8 m), an average depth was used during the plotting of the graphs.

The relative content variations of the mobility index and the other chemical weathering indices with depth for the andesite indicate that significant enrichments of MgO, LoI, WPI, and CEC occur near the surface (Fig. 6a, b). They indicate that the chemical weathering is active especially for the first 3–4 m. It diminishes with depth. The other indices either fluctuate with depth or the variations are not significant. Considering the fact that LoI and CEC measurement using MBA test are cheap and quick methods giving good correlation with the weathering depths of the andesite, the use of these indexes is suggested for the quantification of the weathering depths for andesite.

Pressuremeter tests

A total of 29 Menard Pressuremeter tests were performed in four boreholes (one in Solfasol, one in Ovacik, and two in Pursaklar) for this study. The boreholes were opened using 66 mm diameter continuous flight auger for the purpose of the pressuremeter testing. Deformation

modulus and limit pressure of the weathered andesite were calculated from the tests. However, due to the limited capacity of the pressuremeter and the strength of the andesite, the limit pressure could not be obtained for some test sections. The deformation modulus of the andesite ranges between 3.81 and 101 MPa. The variation of the deformation modulus with depth shows that the weathering zone characterized by relatively low values of the deformation modulus is mainly confined to the upper 7 m of the section, although there exist local fluctuations especially for the Ovacik site (Fig. 7).

Physicomechanical tests

In the Solfasol site, two undisturbed samples were taken from the weathered andesite from 0.5 and 1 m depths. Attempts to obtain undisturbed samples and to perform SPT test from deeper deposits were unsuccessful due to the higher strength of the rock. The core samples obtained after 5 m depth using double tube core barrel were not suitable for uniaxial testing due to sample length inadequacy. Unconsolidated undrained direct shear tests and index soil tests were performed on undisturbed samples. Table 4 summarizes the results of these tests.

In the Ovacik site, two undisturbed samples were taken from 0.5 to 2 m depths. Two SPT tests were performed at 1.5 and 3 m depths by using a rope and pulley system which has 45% energy ratio. 26 and 39 raw blow counts were obtained from the test. After 4 m depth, coring technique was utilized for boring with double tube core barrel. Total core recovery (TCR) of the rock mass is 100% between 4 and 25 m and rock quality designation (RQD) is approximately 75% between 4 and 15 m and 90% between 15 and 25 m depths. The results of the tests performed on the undisturbed andesite samples taken from Ovacik site is given in Table 4. The consolidation tests also performed on two undisturbed samples (Table 5) indicated that the soil is heavily overconsolidated according to the maximum past vertical effective stress (P_p). On the core samples taken between 4 and 20 m depths, uniaxial compression tests were performed by

using electronic transducers for the measurement of axial strain and load. The uniaxial compressive strengths of the andesite range between 248 and 385 kPa at 4–6 m; 334 and 360 kPa at 6–10 m; 415 and 485 kPa at 10–15 m; and 468 and 554 kPa at 15–20 m. The modulus of deformation (E_{50}) values of the rock are 2.3–17.5 MPa at 4–6 m; 23.5 MPa at 6–10 m; 18.4–28.4 MPa at 10–15 m; and 25.7–32.7 MPa at 15–20 m.

In the Pursaklar site, one undisturbed sample (two in total) from each borehole was taken at 1 m depth. SPT tests could not be performed at this site due to the presence of the stronger andesite. After 5 m, coring technique was utilized with double tube core barrel. TCR of the rock mass is 100% between 5 and 25 m in both boreholes and RQD is approximately 75% between 5 and 15 m and 90% between 15 and 25 m in the first borehole. However, in the second borehole, RQD of the rock mass is 60% between 5 and 7 m; 82% between 7 and 15 m; and 93 % below 15 m. The results of the tests performed on the undisturbed andesite samples taken from Pursaklar site are shown in Table 4. For the samples taken from both boreholes corresponding to 5–20 m depths, the uniaxial compression tests were performed. In borehole 1, the uniaxial compressive strengths of the andesite are approximately 592 kPa at 5–8 m; 728 kPa at 8–12 m; 853 kPa at 10–15 m; and 922 kPa at 16–20 m. The modulus of deformation values (E_{50}) of the rock are 28.4–32.3 MPa at 5–8 m; 43.1–54.9 MPa at 8–12 m; 64.4–69.5 MPa at 12–16 m; and 76.3 MPa at 15–20 m. In borehole 2, the uniaxial compressive strengths of the andesite are 506 kPa at 5–7 m; 927 kPa at 7–12 m; and 971 kPa at 12–20 m. The modulus of deformation values (E_{50}) of the rock range between 37.1 and 42.6 MPa at 5–7 m; 89.4 and 124.7 MPa at 7–12 m; and 92.2 and 135.8 MPa at 12–20 m depths.

Seismic refraction studies

For the seismic refraction studies, a multichannel seismogram with a total of 12 P -wave and 12 S -wave geophones was utilized. First arrival times of the P -waves

Table 2 Major element analyses of the andesite

Oxides (%)	Depth (m)			
	0–1	2–3	3–4	6–8
SiO ₂ (%)	57.48	60.45	55.82	61.59
Al ₂ O ₃ (%)	17.08	15.74	19.29	16.43
Fe ₂ O ₃ (%)	4.65	4.44	4.54	4.62
CaO (%)	2.57	3.97	4.67	2.33
MgO (%)	4.44	2.77	3.38	2.25
SO ₃ (%)	0.12	0.11	0.11	0.10
Na ₂ O (%)	0.55	1.25	1.82	0.93
K ₂ O (%)	0.88	1.38	0.83	2.28
TiO ₂ (%)	0.74	0.70	0.89	0.67
LoI (H ₂ O ⁺)	10.90	8.85	8.23	8.17
Total (%)	99.41	99.66	99.58	99.37

Table 3 The chemical weathering indices used in this study

Chemical weathering index	Formula/definition	Reference
Weathering potential index (WPI) (mole-ratio)	$[\text{K}_2\text{O} + \text{Na}_2\text{O} + \text{CaO} - \text{H}_2\text{O}^+] * 100 / [\text{SiO}_2 + \text{Al}_2\text{O}_3 + \text{Fe}_2\text{O}_3 + \text{TiO}_2 + \text{CaO} + \text{MgO} + \text{Na}_2\text{O} + \text{K}_2\text{O}]$	Ruxton 1968
Ruxton ratio (mole-ratio)	$(\text{SiO}_2) * 100 / (\text{SiO}_2 + \text{TiO}_2 + \text{Fe}_2\text{O}_3 + \text{Al}_2\text{O}_3)$	Ruxton 1968
Parker index (mole-ratio)	$\text{SiO}_2 / \text{Al}_2\text{O}_3$	Ruxton 1968
Parker index (mole-ratio)	$[(2\text{Na}_2\text{O} / 0.35) + (\text{MgO} / 0.9) + 2\text{K}_2\text{O} / 0.25] + (\text{CaO} / 0.7) * 100$	Parker 1970
Vogt ratio (mole-ratio)	$(\text{Al}_2\text{O}_3 + \text{K}_2\text{O}) / (\text{MgO} + \text{CaO} + \text{Na}_2\text{O})$	Vogt 1927; Roaldset 1972
Modified weathering potential index (mole-ratio)	$[\text{Na}_2\text{O} + \text{K}_2\text{O} + \text{CaO} + \text{MgO}] * 100 / [\text{Na}_2\text{O} + \text{K}_2\text{O} + \text{CaO} + \text{MgO} + \text{SiO}_2 + \text{Al}_2\text{O}_3 + \text{Fe}_2\text{O}_3]$	Vogel 1975
CIA (mole-ratio)	$[\text{Al}_2\text{O}_3 / (\text{Al}_2\text{O}_3 + \text{CaO} + \text{Na}_2\text{O} + \text{K}_2\text{O})] * 100$	Nesbitt and Young 1982
Lixiviation index (β) (mole-ratio)	$[(\text{K}_2\text{O} + \text{Na}_2\text{O}) / \text{Al}_2\text{O}_3]_{\text{weathered}} / \{[(\text{K}_2\text{O} + \text{Na}_2\text{O}) / \text{Al}_2\text{O}_3]_{\text{fresh}} + (\text{CaO} / \text{MgO})\}$	Rocha-Filho et al. 1985
ACN (mole-ratio)	$[\text{Al}_2\text{O}_3 / (\text{Al}_2\text{O}_3 + \text{CaO} + \text{Na}_2\text{O})] * 100$	Harnois 1988; Harnois and Moore 1988
ALK (mole-ratio)	$[\text{K}_2\text{O} / (\text{Na}_2\text{O} + \text{K}_2\text{O})] * 100$	Harnois and Moore 1988
LoI	H_2O^+ content (in weight) of specimen heated to 900–1,000°C	Jayawardena and Izawa 1994; Esaki and Jiang 1999; Topal 2002
Mobiles index (I_{mob}) (mole-ratio)	$[(\text{K}_2\text{O} + \text{Na}_2\text{O} + \text{CaO})_{\text{fresh}} - (\text{K}_2\text{O} + \text{Na}_2\text{O} + \text{CaO})_{\text{weathered}}] / [(\text{K}_2\text{O} + \text{Na}_2\text{O} + \text{CaO})_{\text{fresh}}]$	Irfan 1996
MI	$(R_p * R'_i) / (R_{\text{pr}} * R'_p)$ R_{pr} : the percentage by weight of the stable constituent in the weathered product; R_p : the percentage by weight of the stable constituent in the parent rock; R'_i : the percentage by weight of non-stable constituent i in the parent rock; R'_p : the percentage by weight of the non-stable constituent i that remains in the weathered product	Ng et al. 2001; Guan et al. 2001
CEC	With methylene blue adsorption test	AFNOR 1980; Topal 1996

WPI weathering potential index, PI product index, R Ruxton ratio, P Parker index, V Vogt ratio, $MWPI$ modified weathering potential index, CIA chemical index of alteration, β lixiviation index, ACN alumina to calcium-sodium oxide ratio, ALK alumina to potassium-sodium oxide ratio, LoI loss on ignition, I_{mob} mobiles index, MI mobility index, CEC cation exchange capacity

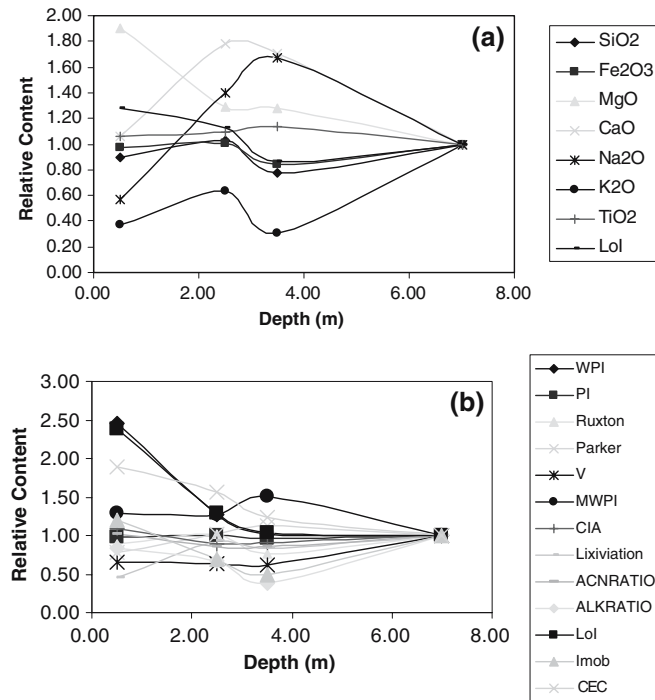


Fig. 6 The relative content variations of (a) the mobility index and (b) the other chemical weathering indices with depth for the andesite

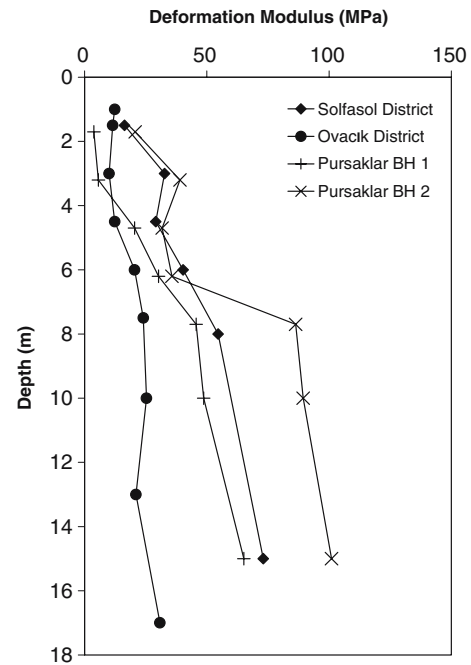


Fig. 7 Variation of the deformation modulus with depth, obtained from the pressuremeter tests

velocities for the weathered zones range between 368 and 1,125 m/s. However, the P -wave velocity increases up to 2,874 m/s for the deeper levels. On the other hand, S -wave velocities vary between 31 and 457 m/s. It reaches a value

Table 4 Laboratory test results of the weathered andesite

Site	Borehole no.	Depth (m)	ϕ	c (kPa)	Soil type	Retaining on no. 4 Sieve	Passing from no 200 Sieve	γ_{natural} (kN/m ³)
Solfasol	1	0.5	22.4	67.7	CH	0.3	54.5	17.5–18.5
		1	30.1	83.3	Not soil	Not soil	Not soil	18–18.5
Ovacik	1	0.5	17.5	31.4	CH	0.3	83.4	16.0–16.5
		2	29.0	27.2	CH	0	93.9	16.0–17.0
Pursaklar ^a	1	1	29.7	54.7	CH	2.7	57.4	16.9–17.7
		2	1	39.1	230.7	CH	3.3	57.9

^aUndisturbed soil samples could not be obtained for deeper levels

were analyzed by using plus minus methods and ray tracing techniques for the determination of the P - and S -wave velocities of the andesite. The data obtained from the seismic refraction survey (Table 6) reveal that P -wave

of 457 m/s for the less-weathered zones. Maximum shear modulus (G_{max}) of the weathered andesite is very low for upper levels (1.9–23.3 MPa) and relatively high (229.8–417.7 MPa) for lower levels.

Table 5 Summary of consolidation tests

Sample	Depth (m)	e_0	w (%)	c_c	c_s	P_p (kPa)
UD 1	0.5	0.918	17.11	0.270	0.096	206
UD 2	2	1.083	11.85	0.223	0.075	314

Rock mass characteristics of the andesite

From surface to downwards, the andesite observed in all three sites has residual soil, completely weathered and highly weathered rocks within the first 25 m. In order to determine the shear strength parameters of the rock

masses from which undisturbed samples could not be taken, geological strength index (GSI) system can be used (Hoek and Brown 1997; Hoek et al. 1998; Hoek and Marinos 2000, 2001). In this study, Hoek and Brown failure criterion (Hoek et al. 2002) was utilized by using GSI system. Figure 8 displays the GSI values assigned to the rock masses by using the field observations. Uniaxial compressive strengths of the intact rocks are taken as 0.6, 0.3, and 0.6 MPa for Solfasol, Ovacık, and Pursaklar sites, respectively, and m_i value is 25. The use of m_i , GSI, and σ_c values yielded nonlinear Hoek and Brown (1997) failure envelopes of the rock masses. By fitting linear regression lines to those of the Hoek and Brown failure envelopes, equivalent Mohr–Coulomb failure envelopes were determined (Fig. 9). For both Ovacık and Solfasol sites, equivalent cohesion intercept and friction angle are found to be 10 kPa and 34° , respectively. However, for the Pursaklar site, 12 kPa equivalent cohesion intercept and 39.6° friction angle are obtained.

Geotechnical evaluation of the site conditions

Based on the findings obtained from both field and laboratory studies, the idealized weathering profile of the andesite is assessed (Table 7). In this profile, the weathered andesite is divided into two main parts. Relatively fresh but deeper levels of the andesite are not considered in this study because the pressure bulb of the domestic buildings is confined within the upper two zones. The profile reveals that the thickness of the residual soil (upper layer) varies for each site characterized by different S -wave velocity, shear strength, and deformation modulus values.

Bearing capacity and settlement problems

For the assessment of the bearing capacity of the weathered andesite, the weakest site according to laboratory direct shear tests and pressuremeter tests, Ovacık, was selected. Meyerhof (1963) method with a factor of safety

of three was preferred in this study because of being one of the most commonly used methods. Three different typical foundations were employed for the bearing capacity calculations and the idealized weathering profile given in Table 7 was used. Table 8 displays the geometry of the foundations generally used in the study area and the allowable bearing capacities. For the calculation of the allowable bearing capacity of the mat foundation, weighted average of the shear strength of two layers was used due to the fact that the failure plane penetrates both the layers. As it is clear from Table 8, the bearing capacity of the weathered andesite is high enough (average pressure of a five storey domestic building is about 100 kPa for a mat foundation) and is not likely to be a problem for light domestic buildings.

The boreholes drilled in the study area were all dry. Thus, the weathered andesite is not expected to completely turn into saturated clay deposits during the lifetime of the buildings. Therefore, the consolidation settlement is not considered to be a major concern. This is also reflected on the consolidation tests performed on the very shallow undisturbed samples taken from Ovacık site, which contains the weakest residual soils (Table 5). In these tests, the maximum past vertical effective stress was calculated as very high when compared to the present vertical effective stress, i.e., soil is heavily over-consolidated. Although the consolidation settlement may not be a major concern, large immediate settlement of the foundations may be expected due to the decreased deformation modulus values caused by weathering.







For the calculation of the immediate settlement, finite difference method with Flac 2D (Fast Lagrangian Analysis of Continua) was utilized because of the layered nature of the weathered andesite. Flac 2D is a finite difference software developed for the non-linear numerical analysis of a two-dimensional continuum body (Itasca 2002). The formulation can accommodate large displacements and strains and non-linear material behavior, even if yield or failure occurs over a large area or if total collapse occurs. The explicit solution scheme gives a stable solution to unstable physical problems. Dynamic equations of motion are used in the Flac

Table 6 The results of the seismic refraction survey

Site	Layer no (thickness)	V_p (m/sn)	V_s (m/sn)	ν (dynamic Poisson's ratio)	G_{\max}^a (MPa)
Solfasol	1 (7 m)	368	108	0.432	23.3
	2	2431	457	0.473	417.7
Ovacık	1 (4–7 m)	1125	280	0.452	15.7
	2	2874	374	0.487	279.7
Pursaklar, near to BH 1	1 (3–6 m)	507	31	0.497	1.9
	2	1683	231	0.486	106.7
Pursaklar, near to BH 2	1 (3–5 m)	760	58	0.496	6.7
	2	1245	339	0.442	229.8

^a G_{\max} maximum shear modulus

Fig. 8 The GSI values assigned to the rock masses

		SURFACE CONDITIONS				
		VERY GOOD	GOOD	FAIR	POOR	VERY POOR
STRUCTURE		DECREASING SURFACE QUALITY →				
	INTACT OR MASSIVE - intact rock specimens or massive in situ rock with few widely spaced discontinuities	90	80		N/A	N/A
	BLOCKY - well interlocked undisturbed rock mass consisting of cubical blocks formed by three intersecting discontinuity sets		70			
	VERY BLOCKY - interlocked, partially disturbed mass with multi-faceted angular blocks formed by 4 or more joint sets		60			
	BLOCKY/DISTURBED/SEAMY - folded with angular blocks formed by many intersecting discontinuity sets. Persistence of bedding planes or schistosity		50			
	DISINTEGRATED - poorly interlocked, heavily broken rock mass with mixture of angular and rounded rock pieces		40			
	LAMINATED/SHEARED - Lack of blockiness due to close spacing of weak schistosity or shear planes		30			
			20			
			10			
		N/A	N/A			

↓ DECREASING INTERLOCKING OF ROCK PIECES

Ovacık and Pursaklar Sites → 25

Solfasol Site → 15

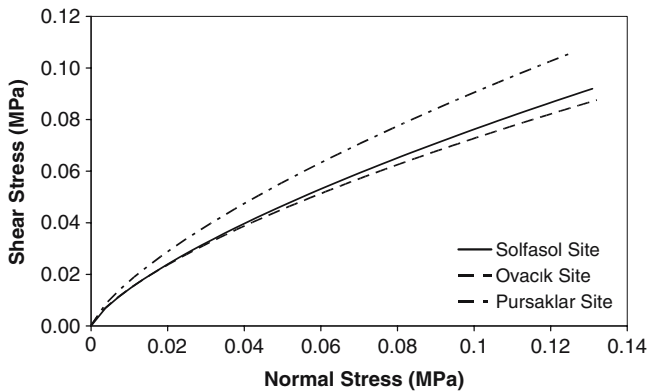


Fig. 9 Hoek and Brown (1997) failure envelopes of the rock masses

algorithm even for the solution of a static problem. Two dimensional version of Flac 2D was utilized for the analyses with linearly elastic perfectly plastic constitutive model. In this model, yielding of the media is modeled with Mohr–Coulomb failure criteria.

For the settlement calculations, the idealized weathering profile given in Table 7 was used. Analyses were performed for mat foundation with 1 m depth and 20 m width; strip foundation with 1-meter depth and 1-meter width. Vertical stress on mat foundation was selected as

100 kPa and on strip foundation 300 kPa, which are typical for five-storey domestic buildings. The finite difference mesh and boundary conditions used for the numerical analyses of mat foundations is shown in Fig. 10. Table 9 summarizes the average settlement (valid for rigid foundations) values for mat and strip foundations on each site. As it can be seen from the table, the average immediate settlement occurred on strip foundations is less than that observed in mat foundations. This phenomenon is due to the limited width of the strip foundation. However, one should bear in mind that in a real foundation system, strip foundations will be in interaction; so settlement should actually be higher than that given in Table 9. The settlement values given in the table are close to the limit values. Therefore, care should be taken for settlement phenomenon when designing foundations. For example, the depth of the foundation may be increased so that the foundation will be on stiffer soils and/or the net pressure of the foundation may be decreased.

Slope instability problems

Shallow slope instability problems are common in the study area (Fig. 11). Therefore, slope stability analyses were performed for hypothetical slopes using Bishop rigorous method. For analyses, circular failure surfaces

Table 7 The idealized weathering profile of the andesite

Site	Layer no. (thickness)	V_s (m/sn)	Shear strength	Deformation modulus, E_{50} (MPa)
Solfasol	1 (7 m)	108	$c = 80$ kPa $\phi = 30^\circ$	25
	2	457	$c = 10$ kPa $\phi = 34^\circ$	50
Ovacık	1 (6 m)	280	$c = 27.2$ kPa $\phi = 29^\circ$	11
	2	374	$c = 10$ kPa $\phi = 34^\circ$	23
	1 (3 m)	31	$c = 54.7$ kPa $\phi = 29.7^\circ$	3.6
Pursaklar	2	231	$c = 12$ kPa $\phi = 39.7^\circ$	Linearly increasing from 5.3 to 65

were assumed and slope stability software “Geostru, Slope Version 8.0” (Geostru 2003) was used with geo-mechanical parameters of the sites given in Table 7. An example of hypothetical slope used in the calculations with 30° angle and 4 m height for Solfasol district, which is rather typical for the site, is given in Fig. 12. Although groundwater was not encountered in the boreholes for all sites, slopes may locally become saturated after a heavy rainy period. For this reason, slope stability analyses were performed under dry and fully saturated conditions. Figures 13, 14, and 15 display the slope angle versus factor of safety relationship for the Solfasol, Ovacık, and Pursaklar sites under dry (a) and fully saturated conditions (b). A factor of safety less than 1.5 is generally achieved only for the steep slopes with a slope height exceeding 8 m. Such a slope does not exist in the study area. The engineering practice in the study area is such that the excavations are confined to the upper 1–2 m, not extending down to 8 m. Therefore, no slope instability problems are expected in the study area.

Ground motion amplification

Due to the reduction of the strength and the shear wave velocity of the andesite associated with weathering, a shift in the predominant site period and amplification of the ground motion around this site period is expected. In

order to determine the ground motion amplification parameters of the selected sites, one dimensional ground response analyses were performed with Shake91. For the prediction of the ground surface motions of flat lying surfaces with horizontally layered soil boundaries, generally one dimensional ground response analyses are used. Shake (Schnabel et al. 1972) is the most commonly used one dimensional ground response analysis software. It utilizes transfer functions and equivalent linear approximation of nonlinear response for the calculation of the ground surface motion. Therefore, it requires the relationships defining the dependency of damping and shear modulus to shear strain. In the literature, there exist several relationships which link shear modulus and

Table 8 The geometry of the foundations and the allowable bearing capacities for the Ovacık site

Foundation type	Depth of foundation (m)	Dimensions of foundation	Allowable bearing capacity (kPa)
Single footing	1	1×1	719
Strip	1	Width 1	500
Mat	1	20×30	2300

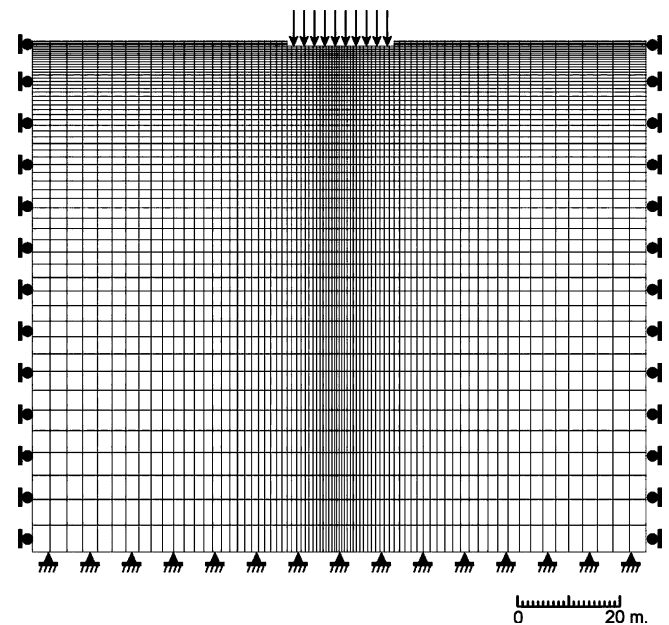
**Fig. 10** The finite difference mesh and boundary conditions used for the numerical analyses of mat foundations

Table 9 Summary of the settlement analyses

Site	Average settlement on mat foundation (mm)	Average settlement on strip foundation (mm)
Solfasol	64	15
Ovacık	145	42
Pursaklar	85	75

damping values of soil to shear strain for various types of soils (Seed and Idriss 1970; Schnabel 1973; Seed et al. 1986; Vucetic and Dobry 1991; Gazetas and Dakoulas 1992). For this study, damping and shear modulus curves of Schnabel (1973) for basement rock, Vucetic and Dobry (1991) for residual soils with plasticity index of 30 were used. Maximum shear modulus values of soil

layers are calculated from the corresponding shear wave velocities.

Earthquake records are needed for Shake analyses. Kandilli earthquake catalogue (Kandilli 2004) was searched to find motions recorded on rock sites having maximum horizontal acceleration approximately 0.1 g. Two records were selected (Figs. 16, 17): these are MDR000 which was recorded in DÜZCE on 11.12.1999 with $PGA=0.12$ g and 531-E which was recorded in DÜZCE on 11.12.1999, with $PGA=0.118$ g. These motions were deconvolved and used for input (base) motion to be taken into account in the shake analyses. Figure 18 presents the results of this calculation for the amplification ratio of the sites. It reveals that the predominant frequencies of the selected sites range between 1.33 and 5 Hz (0.77–0.2 s time period). For Pursaklar

Fig. 11 Shallow slope failure that occurred due to weathering in Solfasol site

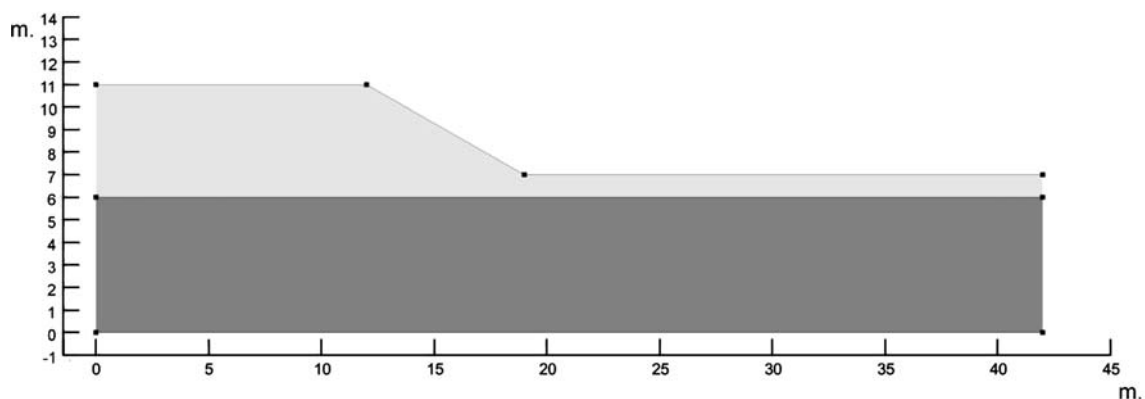


Fig. 12 Hypothetical slope with 30° angle and 4 m height for the Solfasol site

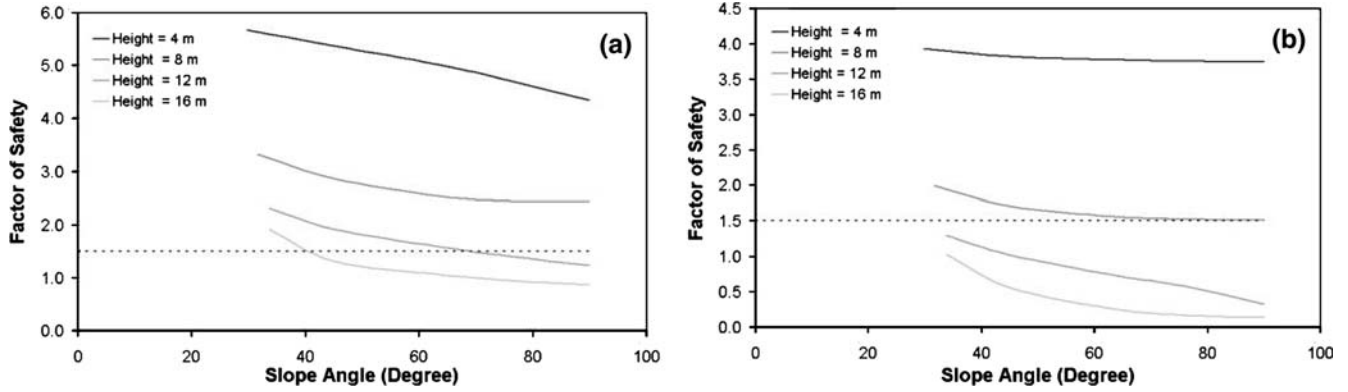


Fig. 13 Slope angle versus factor of safety relationship for the Solfasol site under (a) dry and (b) fully saturated conditions

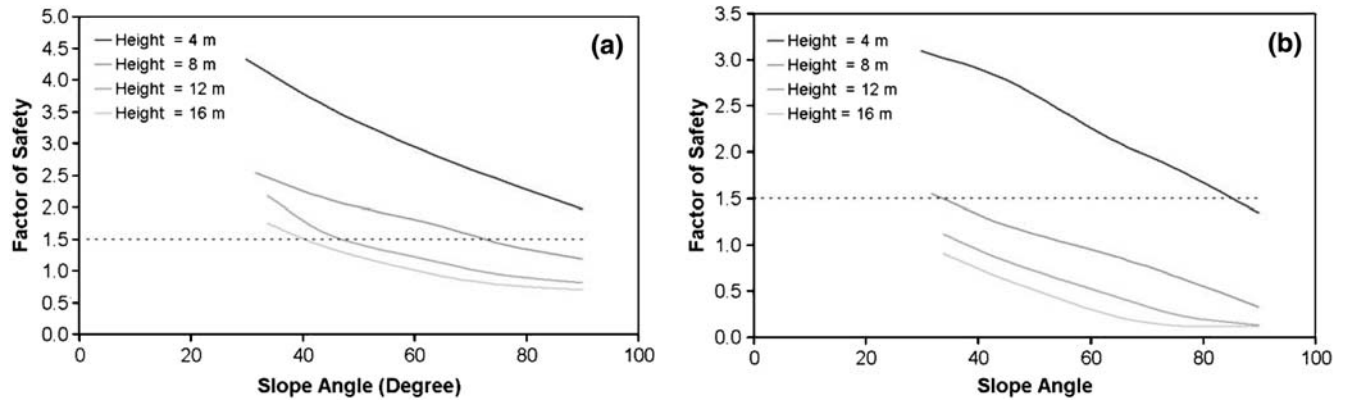


Fig. 14 Slope angle versus factor of safety relationship for the Ovacik site under (a) dry and (b) fully saturated conditions

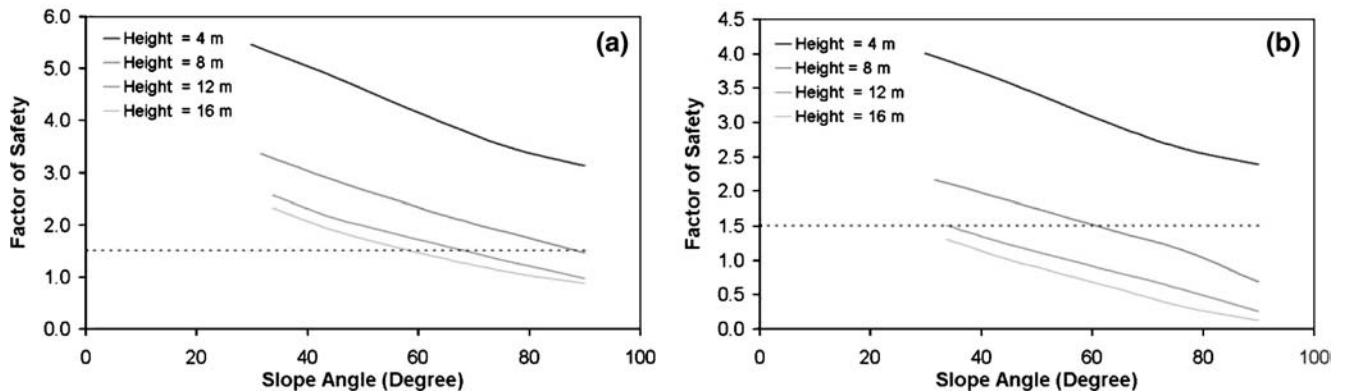
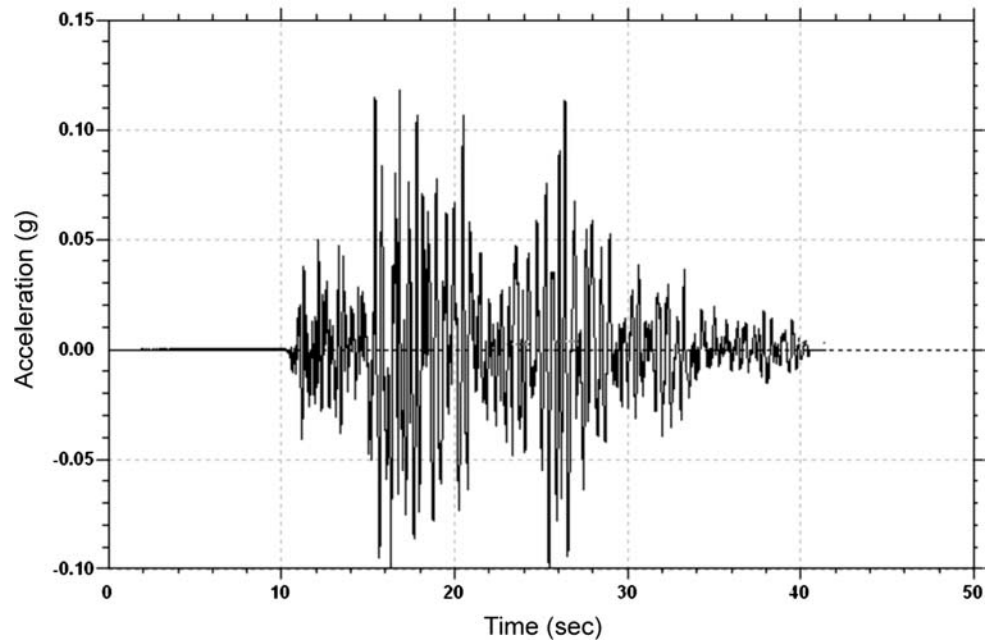


Fig. 15 Slope angle versus factor of safety relationship for the Pursaklar site under (a) dry and (b) fully saturated conditions

site, maximum amplification of 3.7 occurs at the 1.4 Hz (0.71 s), whereas for Solfasol site the maximum amplification (3.8) occurs at the 2.2 Hz (0.46 s). On the other hand, the amplification (4.3) occurs at the 2.6 Hz

(0.38 s) for Ovacik site. The following relationship between the natural period, T_b , and the number of storeys, N , is found to be realistic for damaged buildings in Turkey (Bayulke 1978):

Fig. 16 MDR000 DÜZCE record with PGA = 0.12 g



$$T_b = 0.1N \text{ (damaged)}$$

(1)

Predominant site periods of the Solfasol and Ovacik sites correspond to the predominant period of four and five storey buildings, and the predominant site period of the Pursaklar site corresponds to the predominant period of the seven storey buildings. For a proper earthquake design, the number of stories to be built should be such that the natural period of the building does not match that of the soil column. Based on the soil periods obtained from ground response analyses, it would be

anticipated that buildings with four to seven stories would be severely damaged. Therefore, buildings should be either higher or lower than the indicated stories to avoid resonance problem.

Conclusion

Miocene volcanics including andesite, tuff, and agglomerate cover a large area in Ankara. There exist some geotechnical problems for buildings constructed

Fig. 17 531E DÜZCE record with PGA = 0.118 g

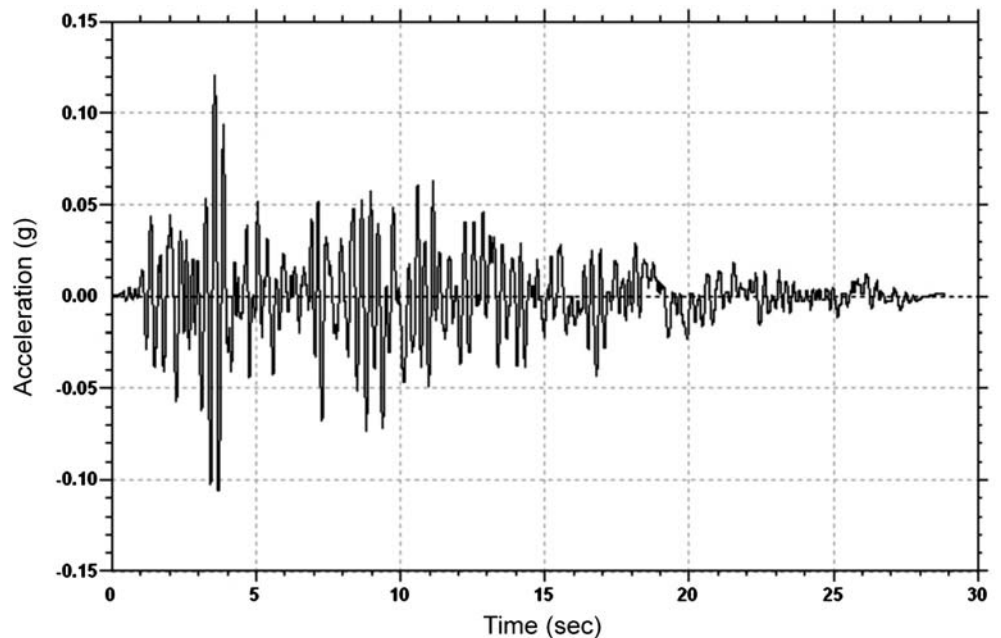
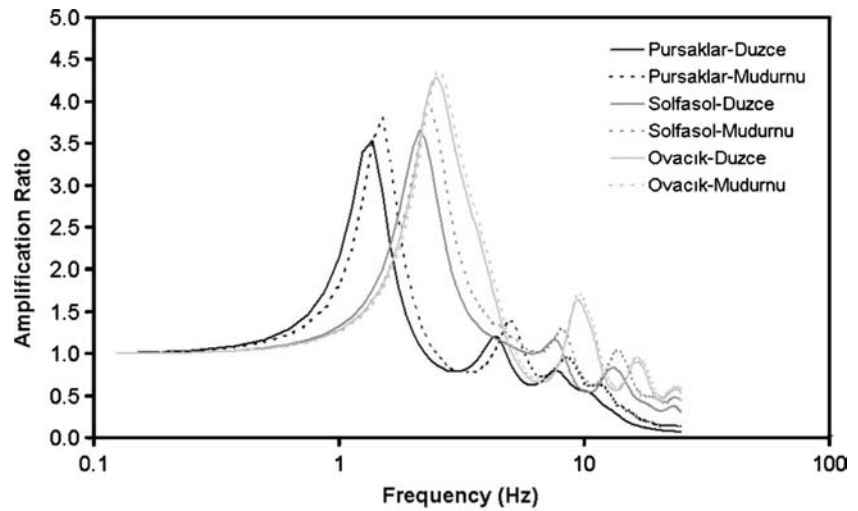


Fig. 18 The amplification ratio of the sites calculated from shake analyses



on the weathered andesite in Ankara. The andesite contains different weathering zones varying from fresh to residual soil. The geomechanical properties of the andesite are adversely affected by weathering. However, the buildings are generally constructed on complexly weathered and residual soil levels of the andesite. In this study, depth of weathering and the variation of the geomechanical properties of the weathered andesite are investigated in three selected sites of Ankara, namely Solfasol, Pursaklar, and Ovacik. Optical microscope, XRD, major element analyses, pressuremeter tests in boreholes, physico-mechanical tests, and seismic refraction method were used for the investigation.

Smectite as an alteration product, feldspar, mica, quartz, hematite, and amorphous silica exist within the samples. The smectite content decreases with depth. The mineralogical and XRD analyses reveal that the weathering is more effective for the upper 2–3 m of the andesite. The chemical weathering indexes indicate a weathering depth of 3–4 m. The weathering zone within the upper 7 m of the andesite has low values of the

deformation modulus with local fluctuations. The seismic refraction method indicates that the upper 3–7 m of the weathered andesite has low seismic velocity. Based on the data obtained, an idealized weathering profile is prepared. The geotechnical analyses reveal that there exist no bearing capacity and consolidation settlement problems in the area. Immediate settlement of the buildings located especially on residual soil may be observed. There may be local and very shallow instability problems, but generally slopes with a height less than 8 m are found to be stable and not expected to cause significant instability problems for buildings. A ground amplification problem exists in the study area. Resonance phenomenon may create problems for buildings especially with four to seven stories. Buildings with four to seven stories should not be preferred in the study area.

Acknowledgments Authors would like to express their thanks to DPT who supported this project and to Mr. Fatih ADIL for his kind efforts during drilling operations.

References

- Abrahamson NA, Silva WJ (1997) Empirical response spectral attenuation relations for shallow crustal earthquakes. *Seismol Res Lett* 68:94–127
- AFNOR (L'Association Française De Normalisation) (1980) *Essai au bleu de methylene*. P18-592. AFNOR 80181. Paris La Defence
- Bayulke N (1978) Behavior of brick masonry structures during earthquakes, *Deprem Arastirma Enstitusu Bulteni*, 6(22):26–41 (in Turkish)
- Boore DM, Joyner WB, Fumal TE (1997) Equations for estimating horizontal response spectra and peak acceleration from western North American earthquakes: a summary of recent work. *Seismol Res Lett* 68:128–153
- Borchardt GA, Harward ME (1971) Trace element correlation of volcanic ash. *Soil Sci Soc Am Proc* 35:626–630
- Borchardt GA, Harward ME, Knox EG (1971) Trace element concentration in amorphous clays of volcanic ash soils in Oregon. *Clays Clay Miner* 19:375–382

- Buyukonal G (1971) Microscopical study of the volcanic rocks around Ankara. Communications Serie C. Sciences Naturales, Torne, 15c
- Campbell WK (1988) Predicting strong ground motion in Utah. In: Hays WW, Gori PL (eds) Evaluation of regional and urban earthquake hazard risks in Utah. USGS Professional Paper, pp 1–31
- Erdik M, Doyuran V, Akkaş N, Gülkan P (1985) A probabilistic assessment of the seismic hazard in Turkey. Tectonophysics 117:295–344
- Esaki T, Jiang K (1999) Comprehensive study of the weathered condition of welded tuff from a historic bridge in Kagoshima, Japan. Eng Geol 55:121–130
- Fukushima Y, Tanaka T (1990) A new attenuation relation for peak horizontal ground acceleration of strong ground motion in Japan. B Seismol Soc Am 80:757–783
- Gazetas G, Dakoulas P (1992) Seismic analysis and design of rockfill dams: state-of-the-art. Soil Dyn Earthq Eng 11:27–61
- Geostru (2003) Slope stability analysis user manual. Geostru Software s.a.s, Italy, 102 p
- Guan P, Ng CWW, Sun M, Tang W (2001) Weathering indices for rhyolitic tuff and granite in Hong Kong. Eng Geol 59:147–159
- Harnois L (1988) The CIW index: a new chemical index of weathering. Sediment Geol 55:319–322
- Harnois L, Moore JM (1988) Geochemistry and origin of ore chemistry formation, a transported paleoregolith in the Grenville Province of Southern Ontario, Canada. Chem Geol 69:67–289
- Hoek E, Brown ET (1997) Practical estimates of rock mass strength. Int J Rock Mech Min Sci 34:1165–1186
- Hoek E, Carranza-Torres CT, Corkum B (2002) Hoek-Brown failure criterion-2002 edition. In: Proceeding of the North American rock mechanics society, Toronto pp 267–273
- Hoek E, Marinos P (2000) A geologically friendly tool for rock mass strength estimation. In: Proceedings of the international conference on geotechnical and geological engineering (Geo-Eng2000), Melbourne, Australia, Technomic Publishing Co Inc., pp 1422–1440
- Hoek E, Marinos P (2001) Estimating the geotechnical properties of heterogeneous rock masses such as flysch. Bull Eng Geol Environ 60:85–92
- Hoek E, Marinos P, Benissi M (1998) Applicability of the geological strength index (GSI) classification for very weak and sheared rock masses: the case of the Athens schist formation. Bull Eng Geol Environ 57:151–160
- Irfan TY (1996) Mineralogy, fabric properties and classification of weathered granites in Hong Kong. Q J Eng Geol 29:5–35
- Irfan TY (1999) Characterization of weathered volcanic rocks in Hong Kong. Q J Eng Geol 32:317–348
- Itasca (2002) Flac2D fast lagrangian analysis of continua in 2 dimensions user's guide, USA
- Jayawardena US, Izawa E (1994) Application of present indices of chemical weathering for Precambrian metamorphic rocks in Sri Lanka. B Ass Eng Geol 49:55–61
- Joyner WB, Boore DM (1988) Measurement, characterization, and prediction of strong ground motion. Earthquake engineering and soil dynamics: 2. Recent advances in ground motion evaluation, ASCE, NY, pp 43–102
- Kandilli (2004) Kandilli seismological data search. Kandilli Observatory and Earthquake Research Institute <http://www.barbar.koeri.boun.edu.tr>
- Kasapoglu KE (1980) Ankara Kenti Zeminlerinin Jeo-Mühendislik Özellikleri, Doçentlik Tezi, Hacettepe University, Beytepe, Ankara, 206 p
- Martin RP (1986) Use of index tests for engineering assessment of weathered rocks. In: Proceedings of the fifth international congress IAEG. Buenos Aires. Balkema, Rotterdam, pp 433–450
- Meyerhof GG (1963) Some recent research on the bearing capacity of foundations. Can Geotech J 1:16–26
- Nesbitt HW, Young GM (1982) Early Proterozoic climates and plate motions inferred from major element chemistry of lutites. Nature 299:715–717
- Ng CWW, Guan P, Shang YJ (2001) Weathering mechanisms and indices of igneous rocks of Hong Kong. Q J Eng Geol 34:133–151
- Parker A (1970) An index of weathering for silicate rocks. Geol Mag 107:501–504
- Roaldset E (1972) Mineralogy and geochemistry of quaternary clays in the Numedal area, Southern Norway. Narsk Geol Tidsskr 52:335–369
- Rocha-Filho P, Antunes FS, Falco MFG (1985) Quantitative influence of the degree of weathering upon the mechanical properties of a young gneiss residual soil. In: Proceedings of the first international conference on geomechanics in tropical lateritic and saprolitic soils. Brasilia 1:281–294
- Ruxton BP (1968) Measures of the degree of chemical weathering of rocks. J Geol 76:518–527
- Sabetta F, Pugliese A (1987) Attenuation of peak horizontal acceleration and velocity from Italian strong motion records. B Seismol Soc Am 77:1491–1513
- Sadigh K, Chang CY, Egan JA, Makdisi F, Youngs R (1997) Attenuation relationships for shallow crustal earthquakes based on California strong motion data. Seismol Res Lett 68:180–189
- Schnabel PB (1973) Effect of local geology and distance from source on earthquake ground motions, PhD. Thesis, University of California, Berkeley
- Schnabel PB, Lysmer J, Seed HB (1972) SHAKE: A Computer program for earthquake response analysis of horizontally layered sites. Report No. UCB/EERC – 72/12, University of California, Berkeley
- Seed HB, Idriss IM (1970) Soil moduli and damping factors for dynamic response analysis, Report No. EERC 70–10, University of California, Berkeley
- Seed HB, Wong R, Idriss IM, Tokimatsu R (1986) Moduli and damping factors for dynamic analyses of cohesionless soils. J Geotech Eng 112:1016–1032
- Suludere Y (1976) Geology of Meşeli – Aşağıemirler – Dedeler (Çubuk Ankara) region. MTA Report No: 6030
- Teoman MB, Topal T, Işık NS (2004) Assessment of slope stability in Ankara clay: a case study along E90 highway. Environ Geol 45:963–977
- Topal T (1996) The use of methylene blue adsorption test to assess the clay content of the Cappadocian tuff. In: Proceedings of the eight international congress on the deterioration and conservation of Stone, Berlin, Vol. 2, pp. 791–799
- Topal T (2002) Quantification of weathering depths in slightly weathered tuffs. Environ Geol 42:632–641
- Ulusay R, Tuncay E, Sönmez H, Gökçeoğlu C (2004) An attenuation relationship based on Turkish strong motion data and iso-acceleration map of Turkey. Eng Geol 74:265–291
- USGS (2005) NEIC: earthquake search: rectangular area. United States Geological Survey http://www.neis.usgs.gov/neis/epic/epic_rect.html
- Vogel DE (1975) Precambrian weathering in acid metavolcanic rocks from the superior province, Villebon Township, South-Central Québec. Can J Earth Sci 12:2080–2085
- Vogt T (1927) Sulitjelmefeltets geologi og petrografi. Nor Geol Unders 121:1–560
- Vucetic M, Dobry R (1991) Effect of soil plasticity on cyclic response. J Geotech Eng 117:89–107